Reducing noise in single-photon-level frequency conversion

Paulina S. Kuo,[1,2,*] Jason S. Pelc,[3] Oliver Slattery,[1] Yong-Su Kim,[1] M. M. Fejer,[3] and Xiao Tang[1]

[1]*Information Technology Laboratory, National Institute of Standards and Technology, Gaithersburg, Maryland 20899, USA*

[2]*Joint Quantum Institute, NIST and University of Maryland, Gaithersburg, Maryland 20899, USA*

[3]*E. L. Ginzton Laboratory, Stanford University, Stanford, California 94305, USA*

Corresponding author: pkuo@nist.gov

We demonstrate low-noise and efficient frequency conversion by sum-frequency mixing in a periodically poled LiNbO$_3$ (PPLN) waveguide. Using a 1556 nm pump, 1302 nm photons are efficiently converted to 709 nm photons. We obtain 70% conversion efficiency in the PPLN waveguide and >50% external conversion efficiency with 600 noise counts per second at peak conversion with continuous-wave pumping. We simultaneously achieve low noise and high conversion efficiency by careful spectral filtering. We discuss the impact of low-noise frequency translation on single-photon upconversion detection and quantum information applications.   © 2013 Optical Society of America

OCIS codes: (230.7405) Wavelength conversion devices; (190.4360) Nonlinear optics, devices; (270.5585) Quantum information and processing.
http://dx.doi.org/10.1364/OL.38.001310

Frequency translation of photons is useful for both classical applications, such as sensitive detection of infrared (IR) photons [1–3], and quantum applications, such as enabling hybrid quantum networks [4–6]. Photon wavelengths can be changed by efficient nonlinear-optical frequency conversion. Converting IR photons to the visible range, where simple and efficient Si avalanche photodiodes (APDs) are available, is attractive for fiber-based quantum communications and sensing. There has been increasing interest in frequency translation for quantum information applications. The quantum state of light, such as its photon statistics and nonclassical correlation properties, can be preserved while its wavelength is changed [4–6]. This process is an enabling technology for hybrid quantum systems [5–7] that combine the storage and processing properties of quantum dots [7], atoms [8], or ions [9,10], with the long-distance transmission capabilities of photons [11]. These systems generally operate at different wavelengths; frequency conversion can be used to match the wavelengths.

In frequency translation, signal photons (at angular frequency ω_s) interact with a strong pump (ω_p) to produce converted photons (ω_c), where $\omega_c = \omega_p + \omega_s$ for upconversion or $\omega_c = |\omega_p - \omega_s|$ for downconversion. The quantum state is preserved in both upconversion and downconversion [4–6,12,13]. Unfortunately, both are affected by undesirable processes that result in noise photons that appear even when there is no signal present. The main noise sources are spontaneous Raman scattering [2,12,14] and spontaneous parametric downconversion [15,16]. Setting $\omega_p < \omega_s$ [2,14,16] and increasing the separation between ω_p and ω_s [13,14] can reduce noise counts. The spectra of noise photons are broad [14,16] compared to that of the signal photons; hence, spectral filtering can reduce noise counts while maintaining high signal conversion. In this Letter, we compare different spectral filtering techniques for achieving low noise [i.e., low dark-count rates (DCRs)] and high system conversion efficiency. We focus on continuous wave (CW) upconversion, but the results can be applied to

downconversion or temporally gated systems. Using a volume Bragg grating filter, we show >50% upconversion efficiency (excluding detector efficiency) with only 600 s^{-1} dark counts at maximum conversion.

We studied upconversion in a periodically poled LiNbO$_3$ (PPLN), reverse-proton-exchanged waveguide [2,14,17]. 1302 nm signal photons were mixed with a strong 1556 nm pump beam to produced 709 nm photons using a PPLN waveguide (52 mm length, 13.5 μm grating period and 30°C temperature). The crystal end facets were antireflection coated for all wavelengths of interest. The waveguide input was fiber pigtailed with free-space coupling for its output. Signal photons were produced by a 200 MHz linewidth, attenuated CW laser, and combined with a 1556 nm CW pump amplified by an erbium-doped fiber amplifier (EDFA) followed by three 1310 nm/1550 nm wavelength-division multiplexers (WDMs) in series to reject any 1302 nm photons generated in the EDFA. An inline polarizer, a polarization controller, and a 1% tap coupler were used to monitor
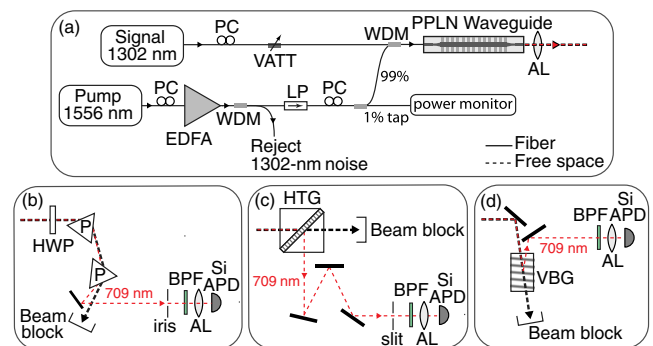

Fig. 1.   (a) Diagram of upconversion setup. The waveguide output is sent to detection stages that filter by (b) a prism pair, (c) a holographic transmission grating (HTG) or (d) a volume Bragg grating (VBG). PC, polarization controller; VATT, variable attenuator; AL, aspheric lens; LP, linear polarizer; BPF, 20 nm bandpass filter; HWP, half-wave plate; P, prism.
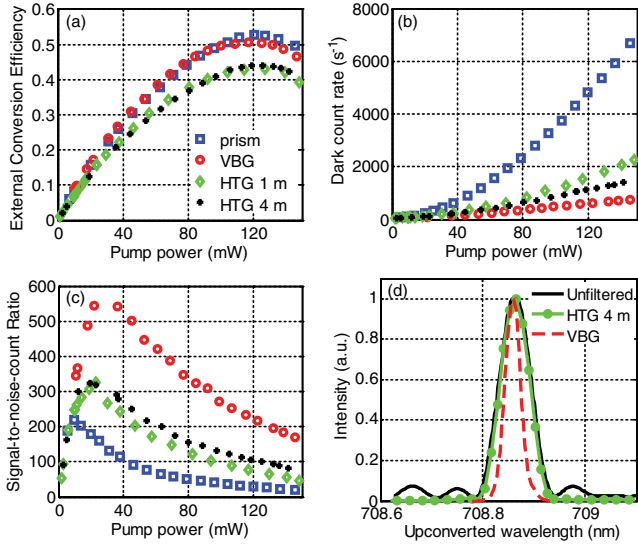
Fig. 2.   (a) External conversion efficiency (not including detector efficiency). (b) DCRs measured by Si APD while signal is blocked. (c) SNCR. (d) Upconversion spectra without filtering, and with filtering by HTG (4 m) and VBG.

the pump power and ensure the polarization did not change as the EDFA power was varied [see Fig. 1(a)].

The output of the PPLN waveguide was filtered with a prism pair, a holographic transmission grating (HTG), or a volume Bragg grating (VBG) (Fig. 1). Upconverted photons were sent to a Si APD (PerkinElmer SPCM-AQR-16) preceded by a 20 nm bandpass filter ($T = 0.93$) that blocked 778-nm second harmonic generated from the pump. The prisms were operated near Brewster's angle for low loss. An iris was placed 10 cm from the second prism to block noise photons. The HTG (Kaiser Optical Systems) diffracted s-polarized, 710 nm light with up to 90% efficiency and produced 0.37°/nm angular dispersion. We tested two path lengths (1 and 4 m) between the HTG and the slit. The VBG (Optigrate) was 11 mm long and designed to reflect near 710 nm with full width at half-maximum (FWHM) < 0.06 nm and diffraction efficiency of up to 95%. The upconverted beam was well collimated with a 1.1 mm $1/e^2$ intensity waist. The slit and iris slightly clipped the upconverted beam (3% reduction in transmission).

We measured external conversion efficiencies (η^{ext}) and DCRs using the different filtering setups. The PPLN waveguide produced 70% maximum conversion efficiency (including input and output coupling losses). The external conversion efficiency [12,13] is the ratio of 709 nm photons just before the Si APD to the 1302 nm photons at the PPLN input (the 65% quantum efficiency

of the Si APD is not included). We set the incident 1302 nm photon rate to 4.17×10^5 s^{-1}, which is comparable to emission rates for quantum dots [12,13]. DCRs were measured by the Si APD with signal photons blocked. We also calculated the signal-to-noise-count ratio (SNCR, the ratio of converted photons to noise photons), which normalizes out the detector efficiency. However, while SNCR is a convenient metric to characterize noise performance, it depends on the signal level (here, set to match quantum dot emission rates).

Figure 2 plots measured η^{ext}, DCRs, and SNCRs. A summary is presented in Table 1. The shapes of the conversion efficiency curves were consistent across the experiments, indicating identical performance of the PPLN waveguide. Since maximum conversion occurred at $P_{\text{pump}} = 120$ mW, the normalized conversion efficiency [2] for the PPLN waveguide was 76% W^{-1}cm^{-2}. While prism filtering had the best external conversion (η^{ext} up to 0.53), it also showed the highest DCR. VBG filtering had simultaneously high external conversion efficiency and low DCR; at maximum conversion, $\eta^{\text{ext}} = 0.51$ with only 600 s^{-1} dark counts. HTG filtering had the same η^{ext} for the 1 and 4 m path lengths, but lower DCRs for the 4 m path. Figure 2(c) plots the SNCRs. Maximum SNCR occurred below the point of maximum conversion. VBG filtering had the best SNCR with 540∶1 between 20 and 35 mW pump power, and 220∶1 SNCR at maximum conversion. At very low pump powers, the DCR approached 50 s^{-1}, which came from intrinsic dark counts of the Si APD and stray light.

Our results show that spectral filtering is an effective technique for reducing noise photons and improving SNCR. Filtering rejects the broadband noise photons that fill the upconversion acceptance bandwidth [2,14,17]. In Fig. 2(d), we show system upconversion spectra measured by fixing the signal to 1302 nm and ≈15 µW power then sweeping the pump wavelength. Without filtering, the PPLN upconversion FWHM bandwidth near 709 nm was 72 pm or 43 GHz. Upconversion spectra using the prisms and HTG (1 m path) filters were identical to the unfiltered curve in Fig. 2(d). Using the HTG with 4 m path length, the sidelobes of the upconversion spectrum were suppressed, while the VBG-filtered spectrum showed further narrowing. We estimated FWHM with the HTG (4 m) to be 66 GHz and with the VBG to be 24 GHz. For applications requiring high speeds or broad bandwidths [7], less narrow spectral filtering or temporal gating may be employed to reduce noise counts.

Having low noise counts in frequency conversion is especially important for quantum information applications where correlations between photons must be preserved.

Table 1.   Comparison of Frequency Upconversion Performance Using Different Filtering Techniques

Filtering Technique	max(η^{ext})	DCR[a] (s^{-1})	max(SNCR)	SNCR[a]	Bandwidth[b]
Prism pair	0.53	4800	220	30	80 nm[c]
HTG (1 m)	0.44	1600	320	70	260 GHz[c]
HTG (4 m)	0.44	1150	320	105	66 GHz
VBG	0.51	600	540	220	24 GHz

[a]At maximum conversion.
[b]Effective filter bandwidth (FWHM).
[c]Estimated from angular dispersion.

The presence of noise photons causes errors and reduced visibility in correlation measurements. For this reason, SNCR is a useful metric. High-fidelity frequency conversion should have SNCR > 1. Taking the VBG example at peak conversion and including detector efficiency, the incident photon flux should be at least $\mathrm{DCR}/\eta = 600~\mathrm{s}^{-1}/(0.51 \cdot 0.65) = 1810~\mathrm{s}^{-1}$ to maintain SNCR > 1.

The requirements for classical applications (such as high sensitivity detection) are different. When only the signal amplitude matters, the background can be subtracted, and system noise comes from shot noise of the dark or background counts. A common metric for detectors is the noise equivalent power (NEP), which is defined as the incident power such that the detected signal is equal to the shot noise [2,18]:

$$\mathrm{NEP} = \frac{\text{dark current shot noise}}{\text{responsivity}}$$
$$= \frac{\sqrt{2eI_D B}}{e\eta/h\nu} = \frac{h\nu}{\eta}\sqrt{2\,\mathrm{DCR}\,B}, \qquad (1)$$

where e is the electron charge, I_D is dark current ($\mathrm{DCR} = I_D/e$), B is bandwidth, η is photon detection efficiency, and $h\nu$ is photon energy. Dividing NEP by the photon energy yields the noise equivalent count rate (NECR):

$$\mathrm{NECR} = \sqrt{2\,\mathrm{DCR}\,B}/\eta. \qquad (2)$$

Using $\eta = 0.51 \cdot 0.65$, $\mathrm{DCR} = 600~\mathrm{s}^{-1}$ and $B = 1~\mathrm{Hz}$, the NECR from Eq. (2) is $105~\mathrm{s}^{-1}$, which is much smaller than the incident count rate needed for SNCR > 1 calculated above. The requirements for high-fidelity quantum state conversion are significantly more demanding than those for low-noise classical light detection.

We show simultaneously high conversion efficiency and low noise-count rates that together produce high SNCR. Previous works have demonstrated low DCRs, but these have been achieved through filtering by a monochromator that also reduced conversion efficiency [19] or by using ultrashort pump pulses with 10^{-4} duty cycle [20]. Recently, quantum-state-preserving frequency conversion has been demonstrated with good efficiency and SNCR. In [13], $\eta^{\mathrm{ext}} = 0.4$ was achieved with SNCR ≈ 100, corresponding to DCR at the detector $\approx 500~\mathrm{s}^{-1}$. Reference [12] observed $\eta^{\mathrm{ext}} = 0.32$ with SNCR ≈ 20. The DCR measured by their detector was $\approx 400~\mathrm{s}^{-1}$, but was partially reduced by the low 12.2% detector efficiency. Our work compares favorably to these results.

In conclusion, we demonstrate that low-noise and high-efficiency frequency translation can be concurrently achieved by incorporating high-transmission, narrow-bandwidth filters, such as VBGs. With VBG filtering, we observed 51% external conversion efficiency and DCR of only $600~\mathrm{s}^{-1}$, corresponding to SNCR of $220\!:\!1$ in a CW system. We note that temporal gating (natural for pulsed systems) can further improve SNCR. This device can be used both for efficient upconversion detection of IR photons, or for quantum-state-preserving frequency conversion of single photons and other quantum light sources.

References

1. A. P. Vandevender and P. G. Kwiat, J. Mod. Opt. **51**, 1433 (2004).
2. C. Langrock, E. Diamanti, R. V. Roussev, Y. Yamamoto, M. M. Fejer, and H. Takesue, Opt. Lett. **30**, 1725 (2005).
3. L. Ma, O. Slattery, and X. Tang, Opt. Express **17**, 14395 (2009).
4. P. Kumar, Opt. Lett. **15**, 1476 (1990).
5. S. Tanzilli, W. Tittel, M. Halder, O. Alibart, P. Baldi, N. Gisin, and H. Zbinden, Nature **437**, 116 (2005).
6. R. Ikuta, Y. Kusaka, T. Kitano, H. Kato, T. Yamamoto, M. Koashi, and N. Imoto, Nat. Commun. **2**, 1544 (2011).
7. K. De Greve, L. Yu, P. L. McMahon, J. S. Pelc, C. M. Natarajan, N. Y. Kim, E. Abe, S. Maier, C. Schneider, M. Kamp, S. Höfling, R. H. Hadfield, A. Forchel, M. M. Fejer, and Y. Yamamoto, Nature **491**, 421 (2012).
8. B. Julsgaard, J. Sherson, J. I. Cirac, J. Fiurášek, and E. S. Polzik, Nature **432**, 482 (2004).
9. R. Blatt and D. Wineland, Nature **453**, 1008 (2008).
10. C. Clausen, I. Usmani, F. Bussières, N. Sangouard, M. Afzelius, H. de Riedmatten, and N. Gisin, Nature **469**, 508 (2011).
11. I. Marcikic, H. de Riedmatten, W. Tittel, H. Zbinden, and N. Gisin, Nature **421**, 509 (2003).
12. S. Zaske, A. Lenhard, C. A. Keler, J. Kettler, C. Hepp, C. Arend, R. Albrecht, W.-M. Schulz, M. Jetter, P. Michler, and C. Becher, Phys. Rev. Lett. **109**, 147404 (2012).
13. S. Ates, I. Agha, A. Gulinatti, I. Rech, M. T. Rakher, A. Badolato, and K. Srinivasan, Phys. Rev. Lett. **109**, 147405 (2012).
14. J. S. Pelc, L. Ma, C. R. Phillips, Q. Zhang, C. Langrock, O. Slattery, X. Tang, and M. M. Fejer, Opt. Express **19**, 21445 (2011).
15. H. Takesue, Phys. Rev. A **82**, 013833 (2010).
16. J. S. Pelc, C. Langrock, Q. Zhang, and M. M. Fejer, Opt. Lett. **35**, 2804 (2010).
17. J. S. Pelc, P. S. Kuo, O. Slattery, L. Ma, X. Tang, and M. M. Fejer, Opt. Express **20**, 19075 (2012).
18. S. M. Sze, *Physics of Semiconductor Devices*, 2nd ed. (Wiley, 1981).
19. H. Kamada, M. Asobe, T. Honjo, H. Takesue, Y. Tokura, Y. Nishida, O. Tadanaga, and H. Miyazawa, Opt. Lett. **33**, 639 (2008).
20. H. Dong, H. Pan, Y. Li, E. Wu, and H. Zeng, Appl. Phys. Lett. **93**, 071101 (2008).